NOTES AND CORRESPONDENCE

Sublimation of Ice Crystals

JON NELSON

Institute of Atmospheric Physics, The University of Arizona, Tucson, Arizona

4 June 1996 and 8 August 1997

ABSTRACT

Recent experiments on the sublimation of single crystals of ice in an atmosphere of air indicate that the sublimation rate is diffusion limited and initially solid prismatic crystals evolve into time-independent shapes similar to confocal ellipses rotated about their major or minor axis (prolate or oblate spheroids). Step formation at crystal edges and vapor diffusion easily explain these observations.

1. Background

The lack of measurements of ice single crystal sublimation in air has resulted in a glaring gap in our knowledge of ice crystal response to nonequilibrium conditions. An early study of solid prismatic ice crystals sublimating in air was by Shaw and Mason (1955). They measured the sublimation rates of the basal and prism faces of single crystals of ice attached to a substrate. Some of their crystals did not sublimate until a certain undersaturation was reached, a result probably due to molecular bonding to the substrate (Nelson and Knight 1997). At undersaturations greater than approximately 10%, the crystal edges rounded. In contrast, Oraltay and Hallett (1989) examined sublimation of dendritic and needle-shaped crystals on a fiber and facing an airstream. They claimed that the ice surfaces were faceted at 10% undersaturation but rounded and later pointed as the undersaturation increased above 20%. Thorpe and Mason (1966) measured the sublimation rates of ice spheres, plates, and dendrites attached to fibers in an airstream, but discussed neither crystal shape evolution nor the mechanism of sublimation. Rounded edges on sublimating crystals have been observed on cirrus crystals (Sassen et al. 1994), blowing snow (Schmidt 1982), ''hollows'' in negative ice crystals (Knight and Knight 1965), and other crystals (Sears 1957; Hudson and Sears 1961; Lubetkin and Dunning 1984).

Beckmann and Lacmann (1982) measured ice sublimation on a substrate in a pure vapor environment. Their crystals remained faceted during sublimation. The rate measurements showed significant scatter with an average sublimation coefficient[1] of 0.1. This value was later shown to be due largely to surface cooling by latent heat loss: the actual sublimation coefficient was likely much closer to one (Nelson 1993).

Authors of current textbooks on cloud microphysics assume various ice crystal sublimation shapes: Pruppacher and Klett (1978) assume that sublimation is the exact reverse of growth, while Young (1993) states that sublimation shapes have more extreme crystal aspect ratios than growth shapes, but can also be more isometric (equidimensional). However, we measured sublimation shapes that differed from those described in these textbooks.

2. Experimental method

A single ice crystal ($\sim$10 μm OD) is formed at the tip of a fine ($\sim$5 μm OD) glass capillary by freezing liquid water inside the capillary. All crystals are grown, then sublimated, in an isothermal chamber containing unstirred air and vapor, with supersaturation controlled by a puddle of aqueous LiCl solution. Because the solution's volume is much greater than the crystal's, the humidity stayed constant during growth and sublimation. Temperature is controlled to within 0.03°C by immersing the chamber in a constant temperature bath. The undersaturation is determined to within 0.03%.

The procedure is to nucleate an ice crystal near the

Corresponding author address: Dr. Jon Nelson, Institute of Atmospheric Physics, University of Arizona, PAS Building #81, Tucson, AZ 85721.
E-mail: nelson@air.atmo.arizona.edu

[1] The sublimation coefficient (also known as evaporation coefficient) equals the ratio of the actual sublimation rate to that predicted, assuming that all molecules striking the surface stick and the surface molecules desorb at their equilibrium rate. The denominator is the maximum possible sublimation rate so the sublimation coefficient must be less than or equal to one.

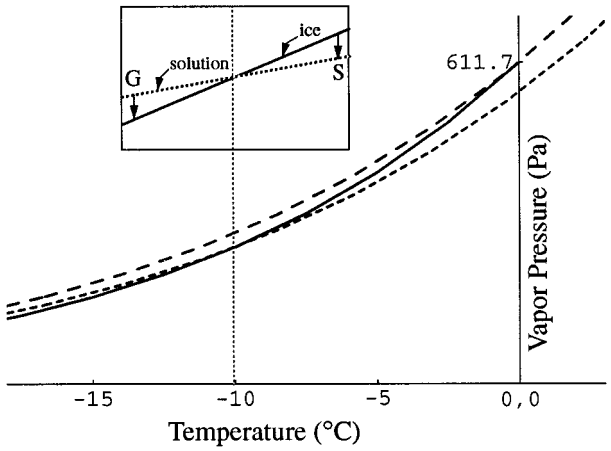

FIG. 1. Equilibrium vapor pressure of ice (solid), liquid water (dashed), and a particular concentration of LiCl in aqueous solution that served as a vapor source/sink (dotted). If the LiCl concentration lowers the freezing point by 10°C, the ice and solution curves cross at −10°C as shown. Sublimation (S) occurs at temperatures above −10°C, while growth (G) occurs below −10°C (inset). By changing the amount of LiCl in the solution, the equilibrium temperature, and hence the degree of under/supersaturation at a given temperature, can be changed.

temperature at which the LiCl solution has the same equilibrium vapor pressure as ice, then lower the temperature to cause vapor flow from solution puddle to crystal (G in inset of Fig. 1), until the crystal is approximately 100 μm, and then raise the temperature above the freezing point of the solution to sublimate the crystal (point S). Approximately 100 crystals were grown and sublimated in this manner, and frequently a single crystal went through several growth/sublimation cycles. Further details of the experimental setup and procedure are in Nelson and Knight (1996).

Compared to previous experiments, the present technique has the following advantages: accurate measure of temperature and humidity, minimal substrate influences on growth and sublimation, and nucleation of only a single crystal. In contrast to growth, the capillary does not appear to influence sublimation (Nelson and Knight 1998, hereafter NK98). Since the crystals were stationary with respect to the surrounding air, our results do not apply directly to large ice crystals in free fall. However, under our simplified environmental conditions, ice crystal sublimation is very reproducible and amenable to theoretical explanation.

3. Results

Ice crystal sublimation was monitored between −18°C and −0.1°C with undersaturations ranging from 0.05% to 5%. We observed that

1) all crystals evolved toward completely rounded shapes,
2) sublimation rates were accurately predicted by the diffusion equation with the surface vapor density at the equilibrium value for a uniform surface temperature,
3) the crystal shape became nearly spheroidal, and
4) the aspect (height to width) ratio remained constant and close to its value at the end of growth.

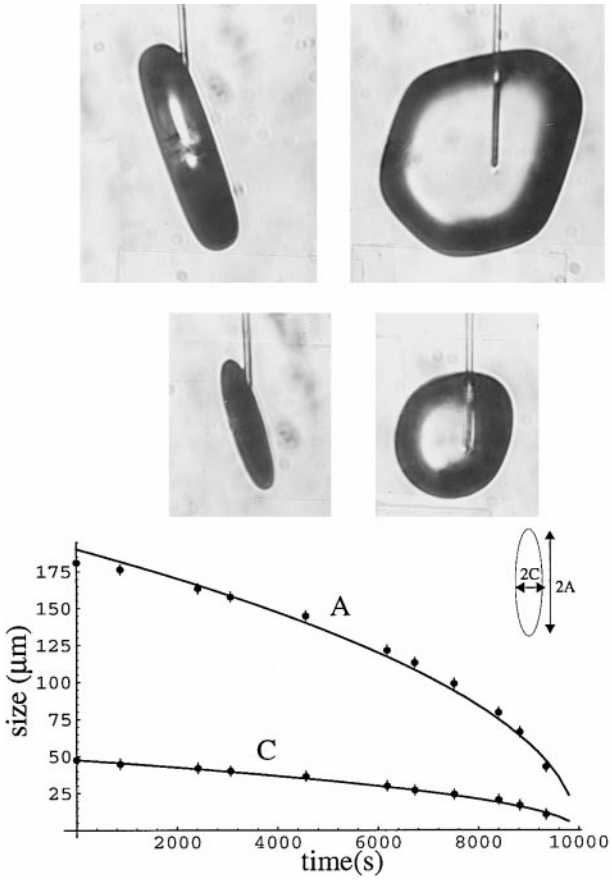

FIG. 2. Sublimation of solid ice crystal at −1.2°C and 1.0% undersaturation. (a) Initial front and side views (top), and 1-h, 14 min later (bottom). (b) Plot of crystal size vs time. Solid line indicates theoretical prediction using spheroid with initial crystal size, aspect ratio, calculated undersaturation, and water vapor diffusion constant; thermal conductivity of air from Pruppacher and Klett (1978); and $\alpha = 1$ (although any value greater than 0.1 would result in nearly the same curve). The diffusion constant of water vapor in air was calculated by measuring the size of an evaporating droplet at −2.3°C and known undersaturation. Error bars here and in the following plots represent uncertainty in measurement size and scale.

These observations are typified by Figs. 2–5.

In Figs. 2–4, we show only crystals above −2°C because they were the most symmetric crystals and remained at constant temperature. Rounding was observed at all measurable undersaturations and temperatures down to −18°C, the lowest temperature studied. Figure 5 illustrates the shape evolution of two crystals and indicates that rounding starts at the surface, then spreads inward to cover the entire crystal surface. It is argued below that this follows from the terrace–ledge–kink

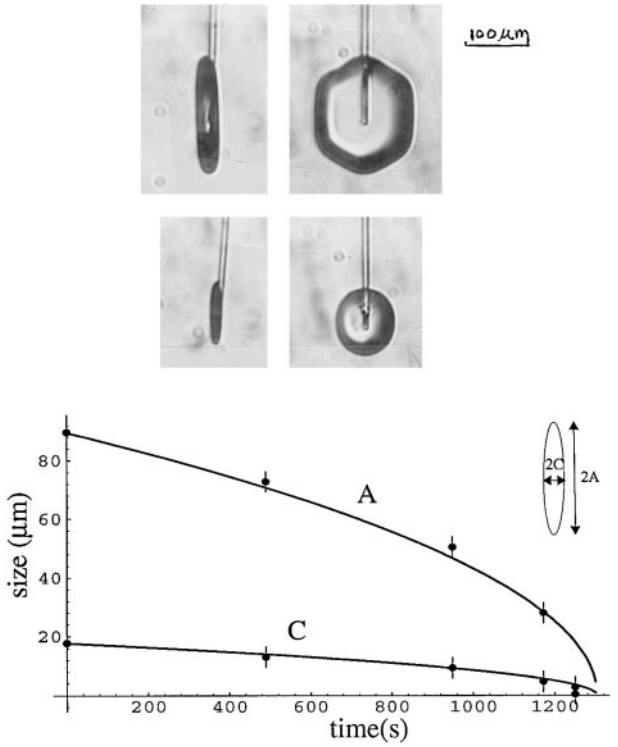

FIG. 3. Sublimation of solid ice crystal at −1.0°C and 1.3% undersaturation. Top: Initial front and side views (top), and 15 min later (bottom). Bottom: Plot of crystal size vs time. Solid line indicates theoretical prediction using the initial crystal size, aspect ratio, and the constants used for Fig. 2.

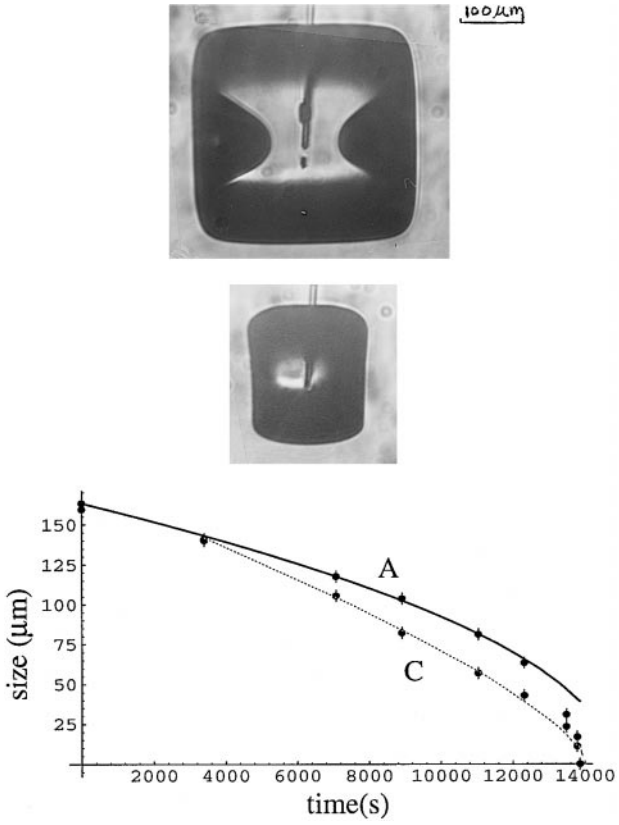

FIG. 4. Same as Figs. 2 and 3 except crystal initially had incomplete basal faces (hollows). Conditions were −0.9°C and 1.4% undersaturation. Dashed line is a hand-fitted curve.

model of crystal surfaces (Burton et al. 1951) and steady-state vapor flow in a diffusion field.

4. Explanation of observations

a. Crystal shape evolution

We assume here that the reader is familiar with the theory of vapor and thermal diffusion from a subliming ice crystal (e.g., Pruppacher and Klett 1978), and instead focus on crystal shape and the role of the surface on sublimation rates because these two factors are needed in the theory.

A rounded crystal surface implies vapor diffusion limited sublimation as follows. The efficiency of surface sublimation is represented by the sublimation coefficient α and for noninteracting molecules migrating on the surface it equals (Burton et al. 1951)[2]

$$\alpha = \frac{2x_s}{l} \tanh\left[\frac{l}{2x_s}\right], \tag{1}$$

where x_s is the mean surface migration distance and l is the step spacing.

Experiments indicate that x_s is of order 10^4 Å (Mason et al. 1963; Sei and Gonda 1989), while comparison of the rounded crystal shapes in Figs. 2–5 to the schematic in Fig. 6 shows that a typical step spacing is less than ~300 Å. Therefore the efficiency of surface sublimation is near 100% (i.e., $\alpha \sim 1$). In steady state, the vapor diffusive flux from the surface ($DN_\infty(\sigma_s - \sigma_\infty)/r$) equals the net rate of surface molecular exchange ($\alpha\bar{v}N_\infty\sigma_s/4$), where D is the vapor diffusion constant, N_∞ the ambient vapor density (number of molecules/volume), σ_∞ the undersaturation far from the crystal surface, r a mean crystal radius, and $\bar{v}$ the mean gas molecule speed. Thus, the undersaturation at the surface, σ_s, is

[2] A step rejects molecules to the neighboring region of effective width $2x_s$ from which they desorb at nearly the equilibrium rate. So, if another step is within $2x_s$ of it, then $\alpha \sim 1$ according to the definition in footnote 1. The removal of molecules from the steps could also reduce the rate of sublimation by adding a small prefactor to the right-hand side of Eq. (1), but in the absence of significant adsorption of impurity, it is likely that this prefactor is approximately one (Cammenga et al. 1981). This is supported by experimental evidence that $\alpha \to 1$ as the steps become close together (Nelson 1993).

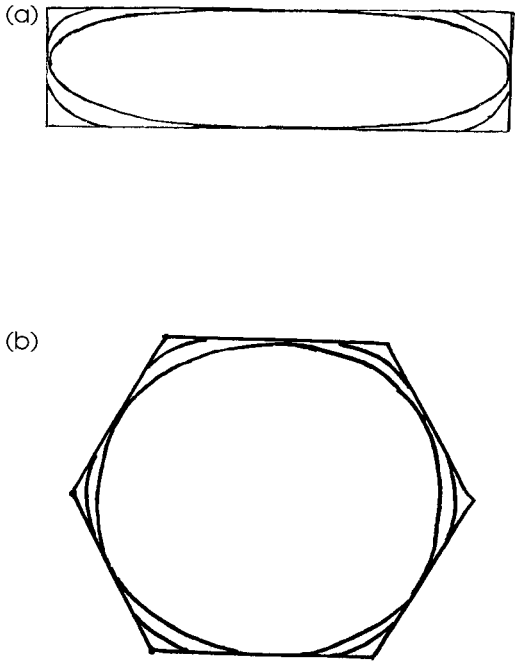

FIG. 5. Sublimation shapes as a function of time: (a) side view of crystal in Fig. 2 at i) initial growth shape, ii) after 50 minutes of sublimation, and iii) after 66 minutes; (b) front view of crystal sublimated at -1.0°C and 1.3% undersaturation for i) initial shape, ii) after 20 minutes of sublimation, and iii) after 36 minutes of sublimation. The shapes at later times were indistinguishable from the last shapes shown in the figures. These figures were obtained by tracing the outline of the crystal's projected image from a negative.

$$\sigma_s = \sigma_\infty \Big/ \left(1 + \alpha \frac{\overline{v}\, r}{4D}\right). \tag{2}$$

[Surface cooling from latent heat loss is neglected in Eq. (2): its omission does not affect the following argument, but it is included in the comparison of measured rate to theory.] With $\alpha \sim 1$, $4D/\alpha\overline{v}$ is nearly the vapor mean free path and equaled approximately 0.2 μm during the experiment. Since r was typically around 100 μm, the second term in the denominator is $\sim$500, so $\sigma_s \ll \sigma_\infty$. Therefore, sublimation is diffusion limited and cannot be influenced by the surface unless α is less than approximately 1/500. From the discussion above, we see that crystal rounding implies diffusion-limited sublimation except in the case of crystals with a size of order of the vapor mean free path, or crystals with a lot of impurity on the surface.

We now explain why a crystal with rounded edges (i.e., a high density of steps at the edges) should evolve into a nearly spheroidal shape of constant aspect ratio.

Soon after a solid crystal becomes undersaturated, the vapor density contours should evolve qualitatively like that shown in Fig. 7 (panels a–d):

(a) The edges are relatively isolated sources of vapor because most steps are here. So the vapor density is larger near the edges as indicated by lines of uniform undersaturation centered around the edges.
(b) As steps sweep across the central part of the face, the vapor source spreads with them. Therefore, lines of uniform undersaturation become more parallel to the surface.
(c) The entire crystal surface becomes an efficient source of vapor (Surek 1972), raising the surface vapor density to near equilibrium. Farther from the crystal, the vapor contours are nearly spherical so the vapor density gradient near the edges is larger (Seeger 1953).
(d) The crystal responds to the larger vapor gradients near the edges by sublimating faster there and thus rounding the crystal.

When $\alpha \sim 1$ (its maximum value) at the crystal edge, the surface cannot remain faceted in a diffusion field (thermal or vapor) because a smaller surface undersaturation at the interior of the face cannot be compensated by a larger α to produce a uniform flux. [A similar phenomenon occurs during growth (Nelson and Baker 1996).] So, the entire face rounds in response to the supersaturation gradient along the surface: the local sublimation rate responds only to the local vapor density gradient, which is determined by local equilibrium. The eventual steady-state shape of the crystal depends on the shape preserving solutions (time independent) of the diffusion equation with a surface vapor density at equilibrium and whether or not the crystal shape can reach one. Ham (1959) showed that spheroids are shape preserving during growth and sublimation if the surface has a uniform temperature.[3] Therefore, if they are also uniquely stable shapes,[4] then the crystal shape should evolve toward that of a spheroid of aspect ratio close to the crystal's initial aspect ratio simply because a stable, steady-state shape is reached before the aspect ratio can significantly change. Figure 5 shows that the crystal shape is a little more blunt at the edge as compared to an ellipse. This deviation from an ellipse could be due to one or more of the following: 1) photograph taken slightly off axis; 2) crystal not being symmetrical; 3) the existence of other, more blunt, stable shapes; 4) adsorption of impurities; and 5) the crystal not reaching steady state. For meteorological applications, small deviations from perfect spheroids are unimportant because prediction of sublimation rates using the known values

[3] The appendix contains a proof of the uniformity of temperature and further description of crystal shapes.

[4] Mullins and Sekerka (1963) showed that sublimation of spheres is completely stable with respect to all shape perturbations. Their analysis is easily extended to prolate and oblate spheroids with the result that the latter shapes are also stable. More general ellipsoids are stable too, but it is not known if other stable shapes between a solid hexagonal prism and spheroid exist.

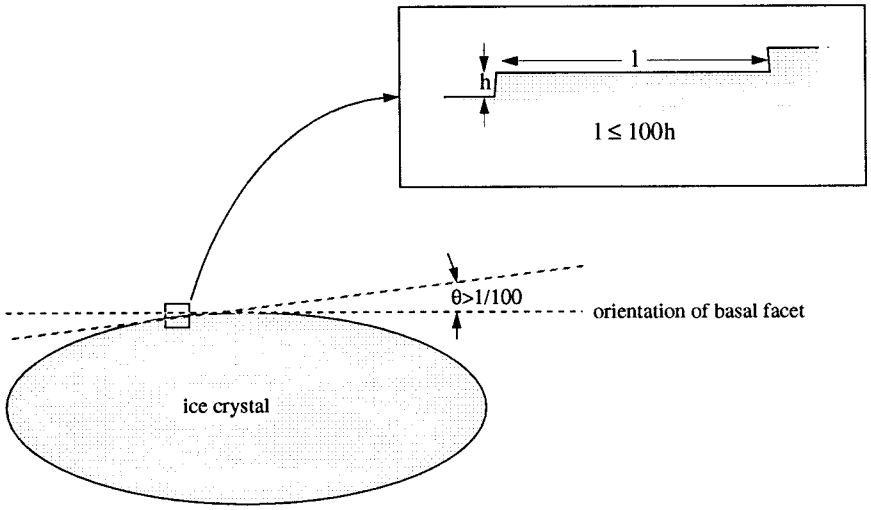

FIG. 6. Magnified schematic drawing of the step spacing on a rounded crystal. The fraction of surface area within 1/100 radian of a basal or prism facet is very small. Defining a step as the boundary of an incomplete layer on the basal or prism face, the typical spacing (l) between steps is less than 100 times the step height (h). So for monomolecular steps with $h = 3$ Å, the step spacing must be less than 300 Å over most of the crystal. Step bunching resulting in larger step heights is not expected during sublimation (Surek 1972) and was not observed.

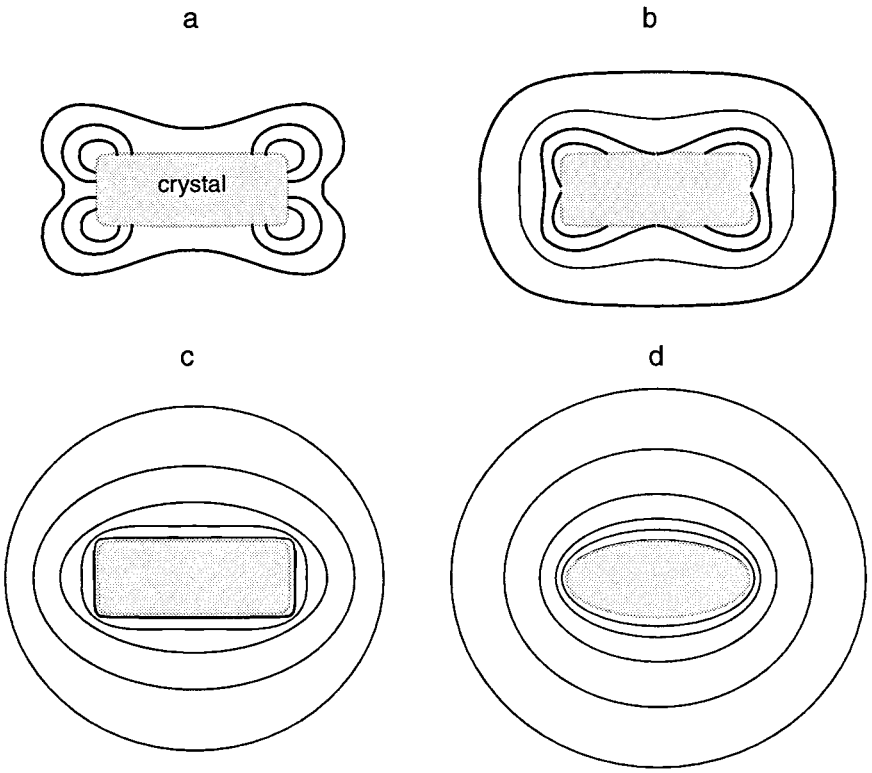

FIG. 7. Schematic drawing of vapor density contours during sublimation. Panels (a)–(c) illustrate evolution of equal vapor density contours as the steps initially migrate inward from the edges. Panel (d) shows the response of the crystal to the resulting nonuniform sublimation flux.

of capacitance for spheroids is accurate as shown in Figs. 2 and 3.

Since closely spaced steps near the edges should lead to both vapor diffusion limited sublimation and near-spheroidal shapes of constant aspect ratio, it only remains to show why the edges should initially produce steps.

b. Mechanism of step formation

Below the thermal roughening temperature of a face (Burton et al. 1951; Leamy and Jackson 1971), crystal sublimation occurs by step motion. The molecules are more weakly bound at the edge, so thermal motion easily dislodges them to create a step on each adjoining face[5] (Fig. 8a left). With the slightest undersaturation, molecules at the step edges should also vibrate loose to a nearby terrace and desorb faster than they are replaced. These steps will sweep inward along the face at a rate linearly proportional to the local undersaturation but inversely related to the local step spacing (Frank 1982). When the step nearest the edge moves a distance such that its direct interaction with edge molecules is negligible (much less than 1 μm), the newly exposed edge molecules can now easily sublimate, thus forming another pair of steps in a continuing process leading to a rounded edge (shown in Figs. 8b,c). Simulations of edge sublimation in a pure vapor predict local rounding near the edge, but most of the crystal face can appear flat (Surek 1972). The faceted shapes of ice crystals sublimating at small undersaturations in a pure vapor observed by Beckmann and Lacmann (1982) agree with Surek's simulations. This argument does not apply to sublimation of negative crystals because the edge molecules are more strongly bound than the ones in the face centers (instead of weaker), which results in facetted sublimation (Knight 1966).

The edge source of steps competes with other step formation mechanisms, such as spirals (Surek et al. 1974) and nucleation of holes (Sears 1957), but these other mechanisms should form steps at slower rates because their curvature requires larger undersaturations for a given step velocity than straight steps from an edge. Step formation from an edge has also been observed on organic crystals (Cammenga et al. 1981).

To summarize, step formation at an edge is a consequence of the geometry of a crystal edge and the kinetics of step motion. In a pure vapor ($4D/\overline{v} \gg r$) the rounded region at the edge can be small compared to the crystal size, but in an atmosphere of air, rounding will spread across the entire surface as described in the previous section.

[5] In fact, there should be many steps.

c. Difference between growth and sublimation

Growth of crystals is different from sublimation due to the difference in ease of step formation. Instead of simply retreating from the edge (Fig. 8, left), growth steps must be built up at some distance (perhaps small) away from an edge. The dominant step formation mechanism for ice is likely the nucleation of new layers (Knight 1972; Frank 1974, 1982; NK98) and is shown on the right in Fig. 8. The high curvatures at the step edge of new embryos reduces their formation rate depending on the step edge energy. This process leads to faceting (Burton et al. 1951; Frank 1982) and, since the step edge energy likely depends on temperature and face orientation, it also leads to the dependence of growth habit on time, temperature, and humidity (NK98). In contrast, the sublimation rate has been found to be completely determined by the rate of vapor diffusion and hence larger than the growth rate for a given deviation from equilibrium. One surprising prediction from this rate difference is that an ice crystal surrounded by vapor density oscillating about equilibrium can sublimate even if the time-averaged undersaturation is zero. The lack of control that the surface has on sublimation is responsible for the differences between growth and sublimation shown in Table 1. Since crystal shapes become more exaggerated during growth but tend to remain constant during sublimation, the crystal shape should become more exaggerated for a given size if it undergoes repeated cycles of growth and sublimation.

5. Application to the atmosphere

There are several important differences between an ice crystal in a cloud and in our experiments. We did not intentionally include airflow or impurities nor did we study hollowed, rimed, or polycrystals. However, the sublimation mechanism that leads to rounded crystal forms in our apparatus should also apply to typical atmospheric environments and lower temperatures. Support for this comes from observations of rounded ice crystals in undersaturated regions of cirrus (Sassen et al. 1994).

When an ice crystal falls in the atmosphere, the airflow around the crystal reduces the size of the diffusion transport region to a thin layer around the crystal (Pruppacher and Klett 1980). Even for large crystals, the sublimation rate will be diffusion limited (Levich 1962) and inversely related to the layer thickness. Since it is likely that this boundary layer is thinnest at the edges where the air flows around the crystal (Ji and Wang 1990), sublimation should be faster at the edges, resulting in rounded crystal shapes for ventilated crystals. Therefore, ventilation is not expected to lead to faceting; however, it might change the aspect ratio.

Since our crystals were grown in unfiltered laboratory air for long periods of time (up to several days) and frequently went through many growth/sublimation cycles, the amount of impurity accumulated on the ice

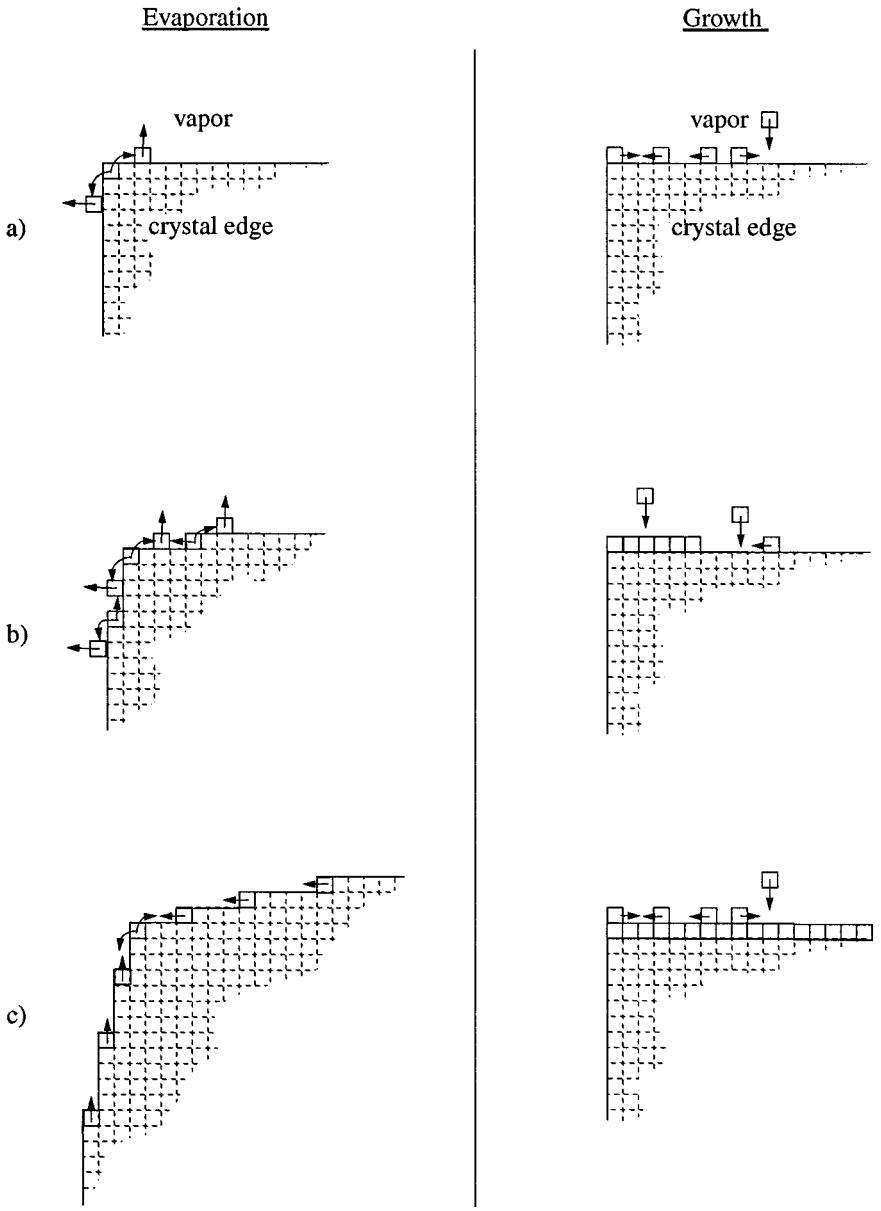

FIG. 8. Schematic drawing illustrating the difference in the generation of steps for sublimation (left) and growth (right). Sequence (a)–(c) is increasing time. The desorption process shown on the left in (a) and (b) is not shown in (c) to avoid cluttering the drawing. The steps are farther apart away from the edge because the first steps across the face increase their speed as they move into step-free regions. The growth mechanism shown on the right is step (or layer) nucleation, which is likely the dominant mechanism for snow crystal growth (Frank 1982; NK98).

surfaces could be comparable to that encountered by an ice crystal in a polluted cloud environment. According to the model of Chen and Crutzen (1994), the equilibrium vapor pressure of the ice could lower by up to 9% under these conditions. Although we could detect 0.5% changes in supersaturation, we did not observe a lowering of the equilibrium vapor pressure. This finding agrees with the analysis in Baker and Nelson (1996). Since sublimation was diffusion limited, we did not detect any impurity effects on the sublimation rate. This contrasts with a reported reduction in sublimation rates in a polluted environment (Diehl et al. 1996) and a possible explanation of long lifetimes of ice crystals in the Arctic stratosphere (Peter et al. 1994). In these latter studies, the ice crystals were in an environment different from our experiment.

Ice crystal growth shapes above $-18°C$ in clouds are rarely solid prisms like those in our study. However, the

TABLE 1. Observed differences between ice crystal sublimation and growth in an atmosphere of air.

Characteristic	Sublimation	Growth
Step motion reduce rates?	no	yes
Shape changes with time?	no	yes
Faceted?	no	yes
Shape depend on temperature?	no	yes
Shape depend on humidity?	no	yes

tendency toward spheroidal shapes should still occur in branched crystals, but the limiting shape might not be reached before the crystal disappears. If the rounding mechanism applies at lower temperatures, then the capacitive spheroid model described by Pruppacher and Klett (1978) and used by several authors (Stephens 1983; Hall and Pruppacher 1976) should accurately describe sublimation of solid polyhedral crystals in colder clouds where they are more common. Hollow and polycrystalline crystals were also observed to round, indicating that $\alpha \sim 1$, but the shapes took much longer to become spheroidal.

The time for an initially solid polyhedral crystal to completely lose all facets, assuming that the rate of mass loss is the same as the mass loss rate from a spheroidal crystal of the same aspect ratio, is calculated to be approximately 50% of the crystal's total lifetime independent of both its aspect ratio and the undersaturation. This estimate is in rough agreement with our observations but has not been sufficiently tested.

In addition to sublimation, there are other possible crystal rounding mechanisms: equilibrium thermal roughening near 0°C (Elbaum 1992; Bennema 1993), a surface coating of solution, kinetic roughening at high supersaturations (Bennema 1993), and latent heat-induced melting of the surface during growth at high temperatures and supersaturation. In addition, frozen droplets retain their rounded appearance until sufficient growth occurs. Therefore, it is not possible at present to infer undersaturated conditions in the atmosphere merely by sampling rounded crystals.

Sublimation rates and shapes of ice crystals influence several important atmospheric situations. The rates are of interest both because the seeding of lower-level clouds from precipitating ice crystals depends on the fall distances of ice crystals (Hall and Pruppacher 1976) and because sublimation of advected ice crystals from cumulonimbus anvils supplies the upper troposphere with water vapor (Udelhofen and Hartmann 1995; Sun and Lindzen 1993; Smith 1992). Ice crystal sizes and shapes determine the light scattering distribution from optically thin ice clouds. Since crystal rounding eventually removes all facets, we expect that optical effects dependent on facets [sun dogs, haloes, arcs, and pillars (Greenler 1980)] should not occur in cloud regions that have undergone significant sublimation. Also, since surface chemical reactions are known to depend on the molecular positions on the surface, chemical reaction rates on sublimating ice crystals might be different from those on growing crystals because they have a much higher density of steps.

Acknowledgments. The experimental work was done at the National Center for Atmospheric Research, which is sponsored by the National Science Foundation. It would not have been possible without support from a DOE Distinguished Global Change Fellowship and a great deal of experimental assistance from Charles Knight. Comments from David C. Rogers were helpful. Special thanks are due to April Dean of Sutter Instruments, Inc., for supplying us with most of our glass capillaries.

APPENDIX

Uniformity of Temperature in Sublimating Spheroids

A proof that prolate and oblate spheroids with surface vapor density at local equilibrium have uniform temperature is given here.

We use the prolate spheroidal coordinates described in Moon and Spencer (1961) and represented by η, θ, ψ.[6] The crystal is a prolate spheroid, so the surface has fixed η, denoted by η_s, with $\eta > \eta_s$ being external to the crystal. The azimuthal coordinate ψ is dropped since the crystal has azimuthal symmetry. In addition, we make the following assumptions: 1) the temperature is continuous, 2) the vapor density and temperature are in steady state, and 3) the surface vapor density $N_s(\theta)$ equals the value at equilibrium for the local surface temperature $T_s(\theta)$.

The general solution for the (shifted) vapor density, $n(\eta, \theta) \equiv N(\eta, \theta) - N_\infty$, is

$$n(\eta, \theta) = \sum_{i=0}^{\infty} C_i Q_i(\cosh\eta) P_i(\cos\theta), \qquad \text{(A1)}$$

where Q_i and P_i are Legendre polynomials (Moon and Spencer 1961). Similarly, the shifted temperature ($T - T_\infty$) external to the crystal is

$$t^+(\eta, \theta) = \sum_{i=0}^{\infty} A_i Q_i(\cosh\eta) P_i(\cos\theta), \qquad \text{(A2)}$$

while the temperature inside the crystal is

$$t^-(\eta, \theta) = \sum_{i=0}^{\infty} B_i P_i(\cosh\eta) P_i(\cos\theta). \qquad \text{(A3)}$$

We must solve for A_i, B_i, and C_i.

At the crystal surface, assumption 1) together with

[6] The crystal has length $2a\cosh\eta_s$, and diameter $2a\sinh\eta_s$, with a characterizing the coordinate transformation. The aspect ratio $\coth\eta_s$ is constant for shape-preserving solutions.

the orthogonality of the Legendre polynomials results in

$$A_i Q_i(\cosh\eta_s) = B_i P_i(\cosh\eta_s). \tag{A4}$$

In steady state, the net heat flux is zero, so the latent heat flux due to the vapor flux leaving the surface $[LD(g_{\eta\eta})^{-1/2}\partial n/\partial\eta|_{\eta_s}$, with L the latent heat per molecule, and $g_{\eta\eta}$ the metric coefficient for η] equals the heat conduction flux from the surface $[-\kappa_A(g_{\eta\eta})^{-1/2}\partial t^+/\partial\eta|_{\eta_s} + \kappa_C(g_{\eta\eta})^{-1/2}\partial t^-/\partial\eta|_{\eta_s}$, with κ_A and κ_C the thermal conductivities of air and ice, respectively]. After some cancellations and use of the orthogonality condition, this becomes

$$-\kappa_A A_i Q_i'(\cosh\eta_s) + \kappa_C B_i P_i'(\cosh\eta_s) = LDC_i Q_i'(\cosh\eta_s). \tag{A5}$$

If we expand the equilibrium vapor density about the value at the average surface temperature, assumption 3) together with the Clausius–Clapeyron equation results in

$$n(\eta_s, \theta) = E + Ft^+(\eta_s, \theta), \tag{A6}$$

where E and F are positive constants. Using orthogonality of the Legendre polynomials and $P_0 = 1$, we have from Eqs. (A1), (A2), and (A6)

$$\begin{aligned} C_i &= FA_i \qquad (i \geq 1), \\ C_0 &= E + FA_0. \end{aligned} \tag{A7}$$

Since Eqs. (A4), (A5), and (A7) or (A8) are systems of three equations with three unknowns, A_i, B_i, and C_i, there is one unique solution for each value of i. When $i \geq 1$, the solution is $A_i = B_i = C_i = 0$. But since E is nonzero, the coefficients are nonzero for $i = 0$. Therefore, only the first term in the expansion of t^- remains and this term has no η or θ dependence. So the temperature is uniform throughout the crystal. It is easily seen that this conclusion holds whenever n is uniform on the surface. For oblately shaped crystals, the oblate spheroid coordinate system is used with the difference that the argument of the Legendre function of η is $i\sinh\eta$ instead of $\cosh\eta$; otherwise, the proof is the same.

REFERENCES

Baker, M. B., and J. Nelson, 1996: Comment on ''Solute Effects on the Evaporation of Ice'' by J. P. Chen and P. J. Crutzen. *J. Geophys. Res.*, **101,** 23 035–23 036.

Beckmann, W., and R. Lacmann, 1982: Interface kinetics of the growth and evaporation of ice single crystals from the vapour phase II. Measurements in a pure water vapour environment. *J. Cryst. Gr.*, **58,** 433–442.

Bennema, P., 1993: Growth and morphology of crystals: Integration of theories of roughening and Hartman–Perdok theory. *Handbook of Crystal Growth 1, Fundamentals Part A: Thermodynamics and Kinetics,* D. T. J. Hurle, Ed., North Holland, 477–582.

Burton, W. K., N. Cabrera, and F. C. Frank, 1951: The growth of crystals and the equilibrium structure of their surfaces. *Philos. Trans. Roy. Soc. London A,* **243,** 299–358.

Cammenga, H. K., H.-J. Petrick, and F. W. Schulze, 1981: Sublimation kinetics of organic molecular crystals. *J. Cryst. Gr.,* **55,** 351–362.

Chen, J. P., and P. J. Crutzen, 1994: Solute effects on the evaporation of ice particles. *J. Geophys. Res.*, **99,** 18 847–18 859.

Diehl, K., S. K. Mitra, and H. R. Pruppacher, 1996: A laboratory investigation on uptake of SO2, HNO3 and HCl by single snow crystal. *Proc. 12th Int. Conf. on Clouds and Precipitation,* Zurich, Switzerland, Int. Comm. Clouds and Precip., and Int. Assoc. Meteor. Atmos. Sci., 1047–1049.

Elbaum, M., 1991: Roughening transition observed on the prism facet of ice. *Phys. Rev. Lett.*, **67,** 2982–2985.

Frank, F. C., 1974: Japanese work on snow crystals. *J. Cryst. Gr.*, **24/25,** 3–5.

——, 1982: Snow crystals. *Contemp. Phys.,* **23,** 3–21.

Greenler, R., 1980: *Rainbows, Haloes, and Glories.* Cambridge University Press, 195 pp.

Hall, W. D., and H. R. Pruppacher, 1976: The survival of ice particle falling from cirrus clouds in subsaturated air. *J. Atmos. Sci.,* **33,** 1995–2006.

Ham, F. S., 1959: Shape-preserving solutions of the time-dependent diffusion equation. *Quart. Appl. Math.,* **17,** 137–145.

Hudson, J. B., and G. W. Sears., 1961: Evaporation of zinc whiskers. *J. Chem. Phys.,* **35,** 1509–1511.

Ji, W., and P. K. Wang, 1990: Numerical simulation of three-dimensional unsteady viscous flow past fixed hexagonal ice crystals in the air—Preliminary results. *Atmos. Res.,* **25,** 539–557.

Knight, C. A., 1966: Formation of crystallographic etch pits on ice, and its application to the study of hailstones. *J. Appl. Meteor.*, **5,** 710–714.

——, 1972: Another look at ice crystal growth habits. *Trans. Amer. Geophys. Union,* **53,** 382.

——, and N. C. Knight, 1965: ''Negative'' crystals in ice: A method for growth. *Science,* **150,** 1819–1821.

Leamy, H. J., and K. Jackson, 1971: Roughness of the crystal–vapor interface. *J. Appl. Phys.,* **42,** 2121–2127.

Levich, V. G., 1962: *Physicochemical Hydrodynamics.* Prentice-Hall 700 pp.

Lubetkin, S. D., and W. J. Dunning, 1984: The kinetics of growth of adamantane crystals from the vapour II. *J. Cryst. Gr.,* **67,** 528–540.

Mason, B. J., G. W. Bryant, and A. P. van den Heuvel, 1963: The growth habits and surface structure of ice crystals. *Philos. Mag.,* **8,** 505–526.

Moon, P., and D. E. Spencer, 1961: *Field Theory for Engineers.* D. Van Nostrand, 600 pp.

Mullins, W. W., and R. F. Sekerka, 1963: Morphological stability of a particle growing by diffusion or heat flow. *J. Appl. Phys.,* **34,** 323–329.

Nelson, J., 1993: Heat conduction problems in crystal growth from the vapor. *J. Cryst. Gr.*, **132,** 538–550.

——, and M. B. Baker, 1996: New theoretical framework for studies of vapor growth and sublimation of small ice crystals in the atmosphere. *J. Geophys. Res.*, **101,** 7033–7045.

——, and C. Knight, 1996: A New Method for Growing Crystals from the Vapor. *J. Cryst. Gr.,* **169,** 795–797.

——, and ——, 1998: Snow crystal habit changes explained by layer nucleation. *J. Atmos. Sci.*, in press.

Oraltay, R. G., and J. Hallett, 1989: Evaporation and melting of ice crystals: A laboratory study. *Atmos. Res.,* **24,** 169–189.

Peter, T., R. Müller, P. Crutzen, and T. Deshler, 1994: The lifetime of leewave-induced ice particles in the Arctic stratosphere, II. Stabilization due to NAT-coating. *Geophys. Res. Lett.,* **21,** 1331–1334.

Pruppacher, H. R., and J. D. Klett, 1978: *Microphysics of Clouds and Precipitation.* Reidel, 714 pp.

Sassen, K, N. C. Knight, Y. Takano, and A. J. Heymsfield, 1994: Effects of ice crystal structure on halo formation: Cirrus cloud

experimental and ray-tracing modeling studies. *Appl. Optics,* **33,** 4590–4601.
Schmidt, R. A., 1982: Properties of blowing snow. *Rev. Geophys. Space Phys.,* **20,** 39–44.
Sears, G. W., 1957: Role of crystal edges in evaporation. *J. Chem. Phys.,* **27,** 1308–1309.
Seeger, A., 1953: Diffusion problems associated with the growth of crystals from dilute solution. *Philos. Mag.,* **44,** 1–13.
Sei, T., and T. Gonda, 1989: The growth mechanism and the habit change of ice crystals growing from the vapor phase. *J. Cryst. Gr.,* **94,** 697–707.
Shaw, D., and B. J. Mason, 1955: The growth of ice crystals from the vapor. *Philos. Mag.,* **46,** 249–262.
Smith, R. B., 1992: Deuterium in North Atlantic storm tops. *J. Atmos. Sci.,* **49,** 2041–2057.
Stephens, G. L., 1983: The influence of radiative transfer on the mass and heat budgets of ice crystals falling in the atmosphere. *J. Atmos. Sci.,* **40,** 1729–1739.
Sun, D.-Z., and R. S. Lindzen, 1993: Distribution of tropical tropospheric water vapor. *J. Atmos. Sci.,* **50,** 1643–1660.
Surek, T., 1972: Molecular phenomena during crystal evaporation. *J. Cryst. Gr.,* **13/14,** 19–26.
——, G. M. Pound, and J. P. Hirth, 1974: Spiral dislocation dynamics in crystal evaporation. *Surface Sci.,* **41,** 77–101.
Thorpe, A. D., and B. J. Mason, 1966: The evaporation of ice spheres and ice crystals. *Brit. J. Appl. Phys.,* **17,** 541–548.
Udelhofen, P. M., and D. L. Hartmann, 1995: Influence of tropical cloud systems on the relative humidity in the upper troposphere. *J. Geophys. Res.,* **100,** 7423–7440.
Young, K. C., 1993: *Microphysical Processes in Clouds.* Oxford University Press, 427 pp.